

Use of Low/Mid-Temperature Solar Heat for Thermochemical Upgrading of Energy, Part II: A Novel Zero-Emissions Design (ZE-SOLRGT) of the Solar Chemically-Recuperated Gas-Turbine Power Generation System (SOLRGT) guided by its Exergy Analysis

Na Zhang¹

Institute of Engineering Thermophysics,
Chinese Academy of Sciences,
Beijing, 100190, P. R. C.
e-mail: zhangna@mail.etp.ac.cn

Noam Lior

Department of Mechanical Engineering
and Applied Mechanics,
University of Pennsylvania,
Philadelphia, PA, 19104-6315

Chending Luo

State Nuclear Electric Power Planning
Design and Research Institute,
Beijing, 100094, P. R. C.

This paper adds an exergy analysis of the novel SOLRGT solar-assisted power generation system proposed and described in detail in Part I of this study (Zhang and Lior, 2012, "Use of Low/Mid-Temperature Solar Heat for Thermochemical Upgrading of Energy, Part I: Application to a Novel Chemically-Recuperated Gas-Turbine Power Generation (SOLRGT) System," ASME J. Eng. Gas Turbines Power, Accepted. SOLRGT is an intercooled chemically recuperated gas turbine cycle, in which solar thermal energy collected at about 220°C is first transformed into the latent heat of water vapor supplied to a reformer, and then via the reforming reactions to the produced syngas chemical exergy. This integration of this concept of indirect thermochemical upgrading of low/mid temperature solar heat has resulted in a high efficiency novel hybrid power generation system. In Part I it was shown that the solar-driven steam production helps improve both the chemical and thermal recuperation in the system, with both processes contributing to the overall efficiency improvement of about 5.6%-points above that of a comparable intercooled CRGT system without solar assist, and nearly 20% reduction of CO₂ emissions. An economic analysis of SOLRGT predicted that the generated electricity cost by the system is about 0.06 \$/kWh, and the payback period about 10.7 years (including two years of construction). The exergy analysis of SOLRGT in this (Part II) paper identified that the main potentials for efficiency improvement is in the combustion, the turbine and compressors, and in the flue gas due to its large water vapor content. Guided by this, an improved solar-assisted zero-emissions power generation system configuration with oxy-fuel combustion and CO₂ capture, ZE-SOLRGT, is hereby proposed, in which the exergy losses associated with combustion and heat dumping to the environment are reduced significantly. The analysis predicts that this novel system with an 18% solar heat input share has a thermal efficiency of 50.7% and exergy efficiency of 53%, with ~100% CO₂ capture. [DOI: 10.1115/1.4006086]

Keywords: hybrid power system, solar heat, CO₂ capture, zero-emissions power generation, exergy analysis

1 Introduction

Part I of this paper published separately [1] described the proposal and detailed analysis and performance of a novel solar-assisted chemically-recuperated gas-turbine power generation system (SOLRGT) described in Fig. 1. This paper contains its exergy analysis that led to yet another novel high-efficiency solar assisted

power generation system that also captures the produced CO₂. A detailed system introduction is thus available in Part I of the paper [1], but is briefly summarized here.

Instead (or in addition) of previously proposed and implemented thermal integration of solar heat into the power generation systems by some physical heat absorption process such as evaporation and recuperation, by which it is converted to internal heat of the working fluid, the solar heat input to SOLRGT is integrated thermo-chemically into the endothermic reactions of reforming, wherewith the thermo-chemical integration converts the absorbed solar heat into the working fluid chemical energy, thus achieving an upgrading of the solar heat for manufacturing a fuel that can then be burned to attain a high temperature.

¹Corresponding author.

Contributed by the International Gas Turbine Institute (IGTI) of ASME for publication in the JOURNAL OF ENGINEERING FOR GAS TURBINES AND POWER. Manuscript received January 21, 2012; final manuscript received February 3, 2012; published online April 20, 2012. Assoc. Editor: Dilip R. Ballal.

Table 2 Exergy analysis result of the SOLRGT cycle (based on 1 kmol/s CH₄)

	[MW]	[%]
EXERGY INPUTS		
Fuel	844.8	91.3
Solar heat	79.9	8.6
EXERGY OUTPUT		
Power generation	461.9	49.9
EXERGY LOSSES		
Combustor (COM)	235.4	25.4
Reformer (REF)	9.3	1.0
Recuperator (REP)	10.8	1.17
GT compressors and turbine	113.5	12.3
Economizer (ECO)	13.9	1.5
Water pump & methane compressor	6.6	0.72
Flue gas	64.5	6.97
Mechanical loss	9.4	1.02

Using Eq. (3) and (6), the replacement of fossil fuel by solar energy is expressed as:

$$R_f = \frac{W_{net}/\eta_{e,ref} - Q_f}{Q_{sol}} = SR_f \cdot \frac{W_{net}/\eta_{e,ref}}{Q_f} \cdot \frac{Q_f}{Q_{sol}} = \frac{SR_f}{1 - SR_f} \frac{1 - X_{sol}}{X_{sol}} \quad (7)$$

Similarly, the replacement of fossil fuel by solar exergy is expressed as:

$$R_{fe} = \frac{W_{net}/\eta_{e,ref} - Q_f}{Q_{sol}(1 - T_0/T_{sol})} = \frac{R_f}{(1 - T_0/T_{sol})} \quad (8)$$

2 Exergy Analysis

An exergy analysis was performed to identify the exergy losses in the SOLRGT system and thereby obtain guidance for further system improvement. The dead state is defined as 25 °C/1.013 bar. The exergy efficiency is defined as Eq. (9).

$$\eta_{ex} = \frac{W_{net}}{E_f + Q_{sol}(1 - T_0/T_{sol})} \quad (9)$$

where E_f is the fuel chemical exergy input. Table 2 presents the key results for the specific fuel input rate of 1.0 CH₄ kmol/s. The solar exergy share $X_{e,sol}$ under these conditions is found to be <9%, much smaller than its thermal share of 20.3% because of its relatively low temperature.

As expected, the largest exergy loss occurs in the combustor, followed in magnitude by the exergy losses of the gas turbine compressors and turbines. In the gas turbine compressors and turbines, the coolant air extraction and re-introduction for blade cooling increases the exergy loss. The flue gas contains latent heat associated with the water vapor (23.7 mol%), and it is exhausted at a relatively high temperature of 163 °C, so the flue gas exergy is also a big exergy loss and takes the third place. Since the calculation of the exergy efficiency in Eq. (9) is based on the absorbed solar exergy, the collector and evaporator inefficiencies are not taken into account in this analysis.

2.1 Exergy Utilization Diagram (EUD). The concept of “energy level,” A , is employed to represent the quality of released or accepted energy for a given process [3,4]. It is defined as the ratio of exergy change to energy change

$$A = \Delta E/\Delta H = 1 - T_0 \cdot \Delta S/\Delta H \quad (10)$$

that shows the effect of enthalpy changes on the concomitant exergy ones.

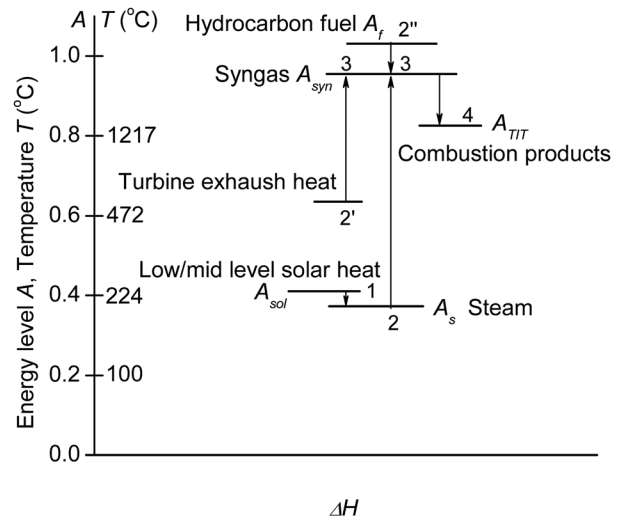


Fig. 2 Upgrading of low-mid temperature solar heat

For the heat transfer process, defining the entropic average temperature as $T = \Delta H/\Delta S$, gives

$$A = 1 - (T_0/T) \quad (11)$$

In this case, A is equivalent to the power produced in a Carnot cycle working between T and T_0 with unit heat input, and is defined as the availability factor or the energy quality [3,4]. The indirect upgrading of the low/mid temperature solar heat can be depicted as shown in Fig. 2.

From 1 to 2 is the process of steam generation, the collected solar heat transforms into the steam latent heat, experiencing the energy level drop from A_{sol} to A_s because of the heat transfer temperature difference. Process (2/2'-3) is the steam reforming process ($CH_4 + H_2O \leftrightarrow CO + 3H_2$). The generated steam at about the temperature of 220 °C with an energy level of about 0.4 is heated, part of the steam takes part in the chemical reaction, the energy level of the steam is elevated partially chemically and partially physically and thus transforms into syngas chemical exergy (from 2 to 3), i.e., from A_s to A_{syn} . At the same time part of the turbine exhaust heat is recuperated by the chemical reaction and converted to the syngas chemical exergy as well (2'-3). The upgrade of the energy levels of both steam and turbine exhaust heat is driven by the energy level drop of the methane that is at about 1.04 to syngas at about 0.96 (depends on its composition) (2''-3). Finally, the process 3-4 is the combustion in which the syngas chemical exergy converts into the internal heat exergy, and the energy level drops to that of the combustion products at the TIT .

Based on the concept of energy level, Jin et al. [5] proposed the graphical exergy analysis method - Exergy Utilization Diagram (EUD) [5]. In each energy-transformation system, the EUD method identifies an energy donor and an energy acceptor. Energy is released by the former and is accepted by the latter as ΔH , and the energy quality of the donor A_d and acceptor A_a are paired. By plotting A_d and A_a versus the transformed energy ΔH , we obtain the exergy loss represented as the area in between. Compared with the $T-Q$ diagram, which interprets the process from the energy point of view, the EUD does it from both the energy and exergy ones: ΔH (or Q) on the abscissa represents the transferred energy quantity related to the first law of thermodynamics; while A on the ordinates denotes the corresponding energy quality (exergy) and is related to the second law of thermodynamic. In addition, $\Delta A = A_d - A_a$ is a parameter that represents the driving force to make the process proceed. This method obviously provides more information than just the exergy difference between the entry and exit states, and is explained and used below for this power system in some detail.

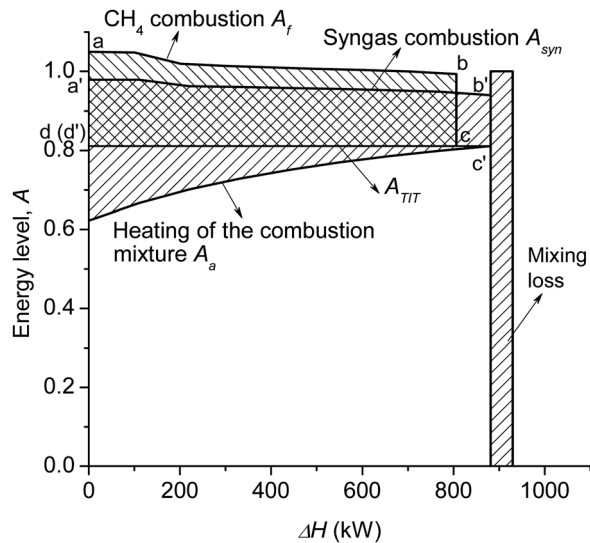


Fig. 3 EUD diagram of combustion process

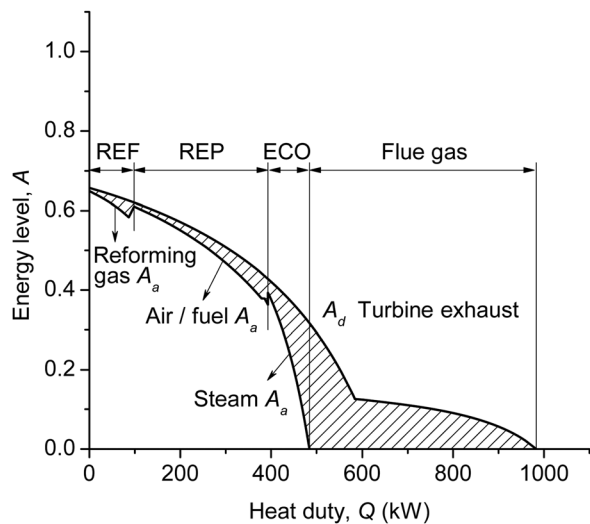


Fig. 4 EUD diagram of turbine exhaust heat recuperation

Figures 3 and 4 show the EUD diagrams for the combustion, and the turbine exhaust heat recuperation process, respectively. The two graphs are drawn in the same scale for easy comparison.

In Fig. 3, the EUD diagram for the combustion process, the oxidation of the unreacted syngas acts as the energy donor (curve A_{syn}), and the heating process of the mixture of reactants and products acts as the energy acceptors (A_a), which are heated to the specific combustion temperature of TIT . The exergy loss by mixing of the reactants is found to be $48.3 \text{ kW}/(\text{mol/s } \text{CH}_4)$ and is indicated by the rectangular area in Fig. 3. With the height of the rectangle being unity, not only its area but also its width represents the amount of the exergy loss of mixing, but one should be aware that the width on the abscissa has nothing to do with the quantity of energy transformed since ΔH for mixing is generally near zero. The exergy loss of mixing is relatively large in this case because of the high fraction of vapor, 68%, in the syngas.

Apart from the mixing loss, the combustion exergy loss is mainly due to the degradation of the high chemical exergy of the fuel (with higher A_f) to the lower exergy of the heat (with much lower A_{TIT}) produced by the combustion (see Refs. [6,7]), as shown by the shaded area between the energy donor and acceptor.

Comparing with direct combustion of hydrocarbon fuel like methane with air, burning of syngas has the following two advantages:

- (1) The reforming-created syngas has higher heating value, as shown in Fig. 3 by the width of the fuel energy donor lines, the heat released is $881 \text{ kW}/(\text{mol/s } \text{CH}_4)$ for syngas combustion (the length of $c'-d'$) and $806 \text{ kW}/(\text{mol/s } \text{CH}_4)$ for methane direct combustion (the length of $c-d$) at the same TIT of 1308°C . Both the recuperated gas turbine exhaust heat and the latent heat of the reacted steam contributed to the heating value increase. For methane fuel flow rate of 1 mol/s , totally 98.6 kW turbine exhaust heat is recuperated in the reformer, of which about 26.5% was converted into physical enthalpy (indicated by temperature rise), and 73.5% is converted into the produced syngas chemical exergy by providing the heat needed for reforming. The $\text{H}_2\text{O}/\text{CH}_4$ mole ratio in the reformer is 6.1, 11.9% of the steam generated by solar heat takes part in the reaction and changes into products, the other 88.1% takes part in the physical heat recuperation and achieves a corresponding energy level elevation as well. The reforming reaction upgrades the absorbed turbine exhaust heat directly, and the low-mid level solar heat indirectly, to the syngas chemical exergy, and then combustion transforms them into the high-temperature thermal heat at energy level of A_{TIT} . The presence of large amount of steam not only serves as a medium for solar heat transformation but also strengthens the methane conversion and lowers the combustion NO_x emissions to a very-low value [8–12].

- (2) The reforming reaction creates syngas that has a lower energy level than methane (by comparing in Fig. 3 the height of line $a-b$ for methane and $a'-b'$ for syngas), so the combustion process of syngas has a lower energy level difference ($\Delta A = A_{syn} - A_{TIT}$) between the energy donor and the energy acceptor. Considering that the temperature, pressure and composition of the combustion products remain approximately the same, the exergy destruction in the conversion from chemical into thermal energy is therefore lower in syngas combustion than that in the unreformed methane fuel, as shown in Figs. 2 and 3. That creates a gain from the combustion of syngas as compared with the direct combustion of methane. In this study, the exergy loss reduction due to syngas combustion (the mixing loss has not been taken into account) is $27.4 \text{ kW}/(\text{mol/s } \text{CH}_4)$, which is equivalent to 3% of the exergy efficiency enhancement, and this profit from combustion of syngas could be expected to increase as the methane conversion rate increases. In the calculations in this paper the methane conversion rate is 37.8%, and higher reforming temperature and steam addition and lower pressure favor the conversion rate, thus showing a direction for reducing the combustion exergy loss.

The EUD diagram of the turbine exhaust heat recuperation process is shown in Fig. 4. As mentioned in Part I [1], the integration of the solar heated steam evaporation process allows the turbine exhaust to be recuperated using only the sensible heat source inside the reformer (REF), the recuperator (REP) and the economizer (ECO) in HRSG, thus obtaining an improved thermal match between hot and cold streams, leading to relatively small exergy loss in these heat exchangers. Totally $484 \text{ kW}/(\text{mol/s } \text{CH}_4)$ heat is recovered in these three heat exchangers with $34 \text{ kW}/(\text{mol/s } \text{CH}_4)$ exergy loss. Flue gas, on the other hand is associated with a high exergy loss of $64.5 \text{ kW}/(\text{mol/s } \text{CH}_4)$, represented by the shaded area in Fig. 4. The flue gas exhausts at a temperature of 163°C , and although it is at an average energy level lower than 0.2, the high mole fraction of water vapor in it associates it with large latent heat loss. As shown in Fig. 4, the water vapor starts a phase change from steam to water at a temperature about 68°C , dumping a large amount of latent heat to the environment. This suggests

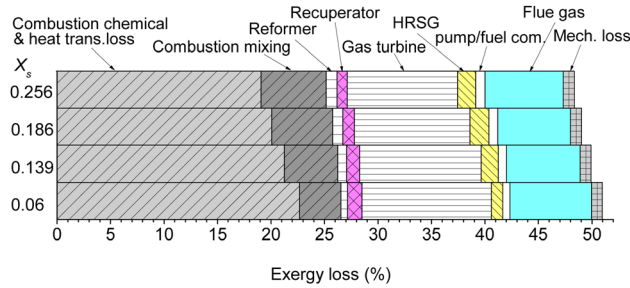


Fig. 5 Exergy losses in the SOLRGT system

that the steam introduction amount is a key parameter to the system performance, and its effect is examined below.

2.2 The Effect of Steam-Air Mass Ratio. Figure 5 shows the exergy loss variation with the steam-air mass ratio X_s . The increase of the amount of added steam, as indicated by increasing X_s , has the following consequences:

- (1) The combustion exergy loss is reduced. In Fig. 5, we separate the combustion exergy loss into two parts, i.e., the exergy loss related to the destruction of chemical exergy and heat transfer, and the mixing loss. As mentioned before, the two-step combustion (reforming and syngas combustion) may reduce the combustion-related exergy destruction compared with the direct methane combustion. Supply of more steam on one hand increases the mixing exergy loss, but on the other hand favors the methane conversion, increasing the syngas production, and the latter dominates, so the overall combustion exergy loss reduced.
- (2) The compressor and turbine exergy loss is reduced. Though increasing water vapor addition increases the turbine working fluid flow and thus requires more blade cooling, the dominant effect is that the increased flow rate of the working fluid produces more power.
- (3) As X_s is increased, this first reduces the flue gas exergy loss till it reaches a minimum at a certain value of X_s and then the loss rises as X_s is increased further. It can be explained by noting that at low X_s there is less water brought into the system, and thus the turbine exhaust heat is not fully recuperated in the HRSG and therefore exhausts at a higher temperature (for example, the flue gas temperature is 210 °C when $X_s = 0.06$), leading to a higher exergy loss to the environment. For high X_s , the exhaust heat is fully recovered thermally by producing more steam, and the flue gas temperature thus decreases. However, the exhaust gas then contains more latent heat associated with the large amount of water vapor (exhausting at 100 °C, the water vapor mole fraction is 34.3% in the flue gas when $X_s = 0.256$), leading to an increased exergy loss to the environment as well.

2.3 Exergy Analysis Results Guidance for System Improvement. From these observations we can conclude that for lower X_s the flue gas exergy loss is mainly associated with the sensible heat loss, indicating that heat recuperation was not fully exploited. Hence, using the unused part of the exhaust heat to replace part of the solar heat for the water evaporation reduces the solar heat use, thus reducing the required collector area. This leads to a significant reduction in the plant investment cost since the solar collectors generally accounts for 40–50% of the capital cost for the entire investment in a solar thermal power plant [1,2]. This reduction of the solar heat input comes from the exhaust heat recuperation rather than from a higher fossil fuel input. Figures 6 and 7 show the effect of replacing part of the solar energy with

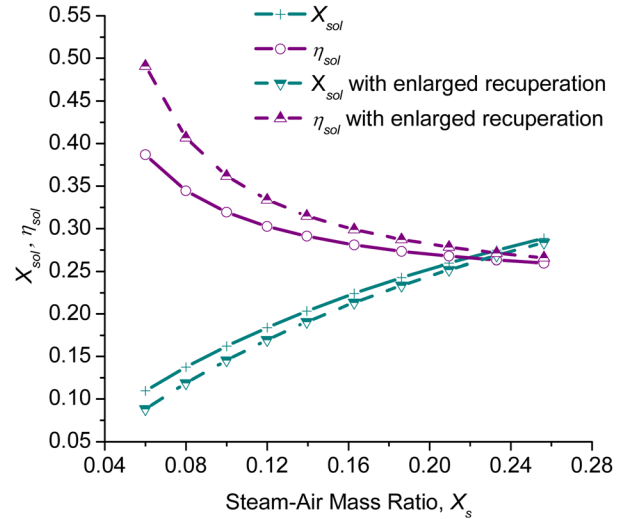


Fig. 6 The effect of enlarging turbine exhaust heat recuperation on the solar thermal share X_{sol} and the solar-to-electricity efficiency η_{sol}

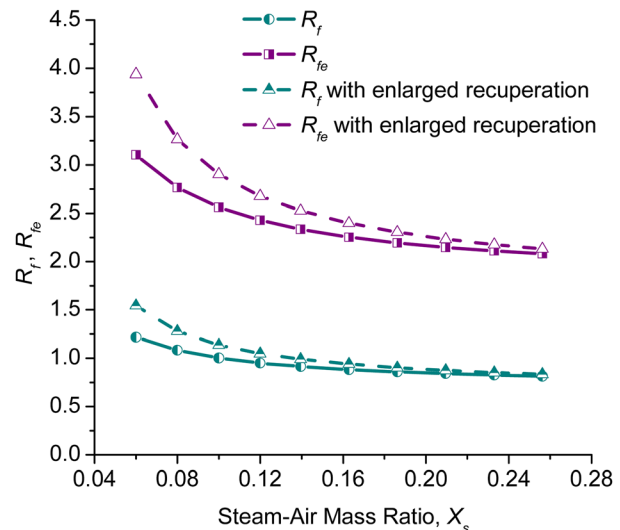


Fig. 7 The effect of enlarging turbine exhaust heat recuperation on the replacement of fossil fuel, R_f and R_{fe}

the excess exhaust heat. We note that increasing the exhaust heat recuperation reduces only the solar energy input share and has no impact on the power generation and fossil fuel input rates; it therefore improves the system overall performance, decreasing the solar heat share while increasing the solar-to-electricity and the global system efficiencies, and also the replacement of fossil fuel by solar energy/exergy, R_f and R_{fe} . The system performance gain is higher in the low X_s region, where more excess sensible exhaust heat is available.

The net solar-to-electricity efficiency reaches the remarkably high value of 49% at $X_s = 0.06$, the replacement of fossil fuel by solar energy/exergy, R_f and R_{fe} , reach 1.5 and 3.9, respectively, at $X_s = 0.06$, and the system exergy efficiency increases by an average 0.5%-points with the increased turbine exhaust heat recuperation.

For high X_s , the flue gas contains a high fraction of steam, and the exergy loss is mainly associated with much latent heat dumped to the environment. This suggests that the exergy loss may be reduced by recycling part of the flue gas to bring its latent heat back to the combustor as done in some oxy-fuel combustion

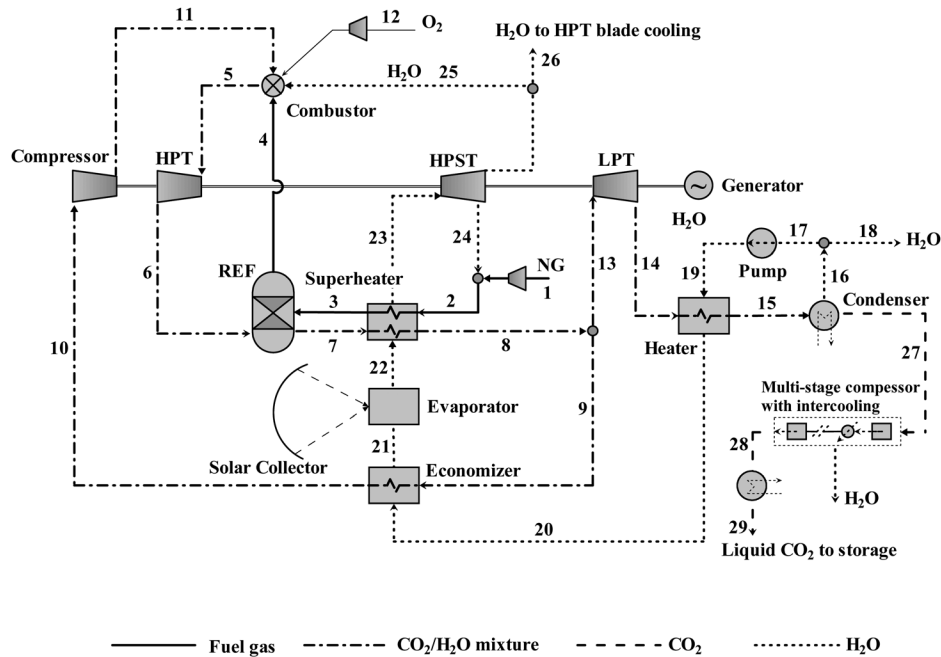


Fig. 8 Process flowsheet of the ZE-SOLRGT cycle

power systems. Thus the exergy analysis of SOLRGT led us to consider replacing the air-based combustion in SOLRGT by oxy-fuel combustion, which has often been considered to accomplish more effective CO₂ capture, and which would thus also add another important positive attribute to this power generation. Either H₂O or CO₂ can be used in the oxy-fuel system as the main working fluid, and the combustion flue gas is also a mixture of H₂O and CO₂. Since the steam fraction in the flue gas is very high already in the SOLRGT system, it is advantageous to choose H₂O as the main working fluid. Beside reduction of the flue gas exergy loss and the ability to capture CO₂, further consideration for selecting steam as the working fluid and oxy-fuel combustion includes: (1) the steam cycle has the advantage of high pressure ratio and low back-power ratio, (2) solar heat collection can easily be integrated for steam generation, (3) steam can be used for high-temperature turbine blade cooling, and the required coolant amount is reduced because of the higher heat capacity of steam than that of air, and especially, (4) the mixing exergy loss in combustion will be reduced when the reformed syngas (which is enriched with steam) mixes with steam working fluid rather than with air.

As shown in Fig. 8, an oxy-fuel cycle (named ZE-SOLRGT by us) is thus proposed, which employs steam as the main working fluid. A Graz-like cycle [13–15] is adopted as the core of the power system, where the main advantage of this configuration is the combination of a high-temperature Brayton top cycle with a high pressure ratio Rankine-like bottom cycle. In Refs. [16,17] the senior 2 authors have proposed and explored the coupling of fuel reforming with a Graz cycle, and achieved an efficiency improvement of about 3%-points.

As shown in Fig. 8, there are three turbines in the system in the Graz-part of the cycle, HPT, LPT and HPST. The high temperature combustion gas first expands in HPT to generate power, and then its exhaust heat is recuperated by reforming and steam superheating in turn. Only part of the flue gas is further expanded in LPT to vacuum and then condensed in the Rankine-like cycle, the remainder is recycled back via a compressor to the combustor without phase change and latent heat release. The non-condensable gases from the condenser are compressed and the combustion-generated CO₂ is captured. The recycled water is pumped to a high pressure of 150 bar and evaporated and superheated, with the produced steam expanded in HPST to generate additional power.

The steam needed for reforming is extracted at the proper pressure from HPST to mix with CH₄ to produce syngas in the reformer, which serves as the fuel to the combustor. Open-loop steam cooling is adopted for the HPT blade cooling, and the coolant steam is bled from the HPST turbine outlet. The remaining HPST exhaust steam is injected in to the combustor as done in the Graz cycle, but this is optional. For the calculations in this paper, all of the HPST exhaust except that needed for HPT blade cooling is sent to the reformer to increase the H₂O/CH₄ ratio in the reforming reaction.

The solar heat is input upstream of the steam superheater. The collected solar heat provides heat for water evaporation. Since the generated steam is at a much high pressure of 150 bar with a saturation temperature of 341 °C, a correspondingly higher solar heat temperature is required than in the SOLRGT system.

We note that the following energy and exergy analyses of ZE-SOLRGT also take into consideration the energy and exergy required to produce the needed oxygen, based on [13–17]. The exergy analysis results in Table 3 suggests that with the same fossil fuel input, the exergy efficiency of the ZE-SOLRGT cycle is 53% with 100% CO₂ capture, remarkably more than 3%-points higher than that of SOLRGT without CO₂ capture. The combustion exergy loss drops from 235.4 kJ/(mol CH₄) in SOLRGT to 206.1 kJ/(mol CH₄) in the ZE-SOLRGT cycle, which includes a mixing exergy loss drop from 48.3 kJ/(mol CH₄) to 33.3 kJ/(mol CH₄). The drop of the mixing exergy in the ZE-SOLRGT system is mainly because of the similarity of the stream compositions before mixing, since both the syngas and the recycled working fluid from the compressor are H₂O-enriched streams.

Another big improvement is attained in the compressor and turbines, in which the compressor consumed only 26.3% of the turbine generated power, compared with 34.8% in the SOLRGT cycle. In the ZE-SOLRGT cycle, the recycled working fluid that is compressed by the compressor is only 59% of the HPT turbine exhaust fluid and the compressor ratio is about 15. The mole flow rate pumped by the pump (Fig. 8) is about half of the working fluid compressed by the compressor; however, the pump has a much higher pressure ratio, of about 1900, with the resulting advantage of much less consumed work. The high-temperature turbine blade cooling with steam rather than air reduces the amount of needed coolant because of higher specific heat of

Table 3 Exergy analysis result of the ZE-SOLRGT cycle (based on 1 kmol/s CH₄)

	[MW]	[%]
EXERGY INPUTS		
Fuel	844.8	90.3
Solar heat	90.9	9.7
EXERGY OUTPUT		
Power generation	496.1	53.0
O ₂ production	56.1	6.0
EXERGY LOSSES		
Combustor (COM)	206.1	22.0
Reformer (REF)	7.26	0.78
Recuperator (REP)	9.0	0.96
GT compressor and turbines	71.0	7.6
Economizer (ECO) and heater	9.4	1.0
Water pump & methane compressor	6.5	0.69
O ₂ compression	1.31	0.14
CO ₂ compression	35.2	3.76
Condenser	38.9	4.16
Mechanical loss	10.1	1.08

steam. In the ZE-SOLRGT system, the ratio of the coolant steam mass flow rate to the turbine inlet working fluid mass flow rate is 13% compared with 17% in the SOLRGT cycle.

The reduction of the exergy loss to the environment is also significant. In the SOLRGT system, the flue gas related exergy loss is as high as 64.5 kJ/mol CH₄, while in the ZE-SOLRGT system, the exergy loss in the condenser is only 38.9 kJ/(mol CH₄) because the condensation releases heat at a relative low temperature of 35 °C. In addition, 59% of the HPT exhaust working fluid is recycled, taking its latent heat back to the combustor; thus significantly reducing the condenser load.

The ZE-SOLRGT system exhibits a thermal efficiency of 50.7% and equivalent exergy efficiency (Eq. (2)) of 55.5%, with ~100% CO₂ capture and 18% solar heat input share. The performance is far better than that of a gas-steam combined cycle at the same *TIT* level, in which the thermal efficiency drops to about 46–48% when using a chemical absorption process for flue gas capture and accomplishing only about 90% CO₂ capture. Further details about the analysis of the ZE-SOLRGT system can be found in Ref. [18].

3 Concluding Remarks

A hybrid solar improved CRGT (“SOLRGT”) system, which integrates power generation with solar heat thermal and thermochemical conversion has been proposed in Part I of this study [1]. In this paper, an exergy analysis was conducted to identify the exergy loss in each main component and the potential for improvement, and the major exergy losses were found to be in the combustion, the turbine and compressors, and in the flue gas exhaust, which also incurs large exergy loss due to its large water vapor content that thus loses the latent heat and its exergy to the environment. Guided by the exergy analysis results, an improved cycle configuration with oxy-fuel combustion and CO₂ capture (named “ZE-SOLRGT”) is thus proposed, with steam as its main working fluid. Its power section is configured on a Graz-like cycle to take advantage of the combination of a high-temperature Brayton top cycle with a high pressure-ratio Rankine-like bottom cycle. After expanding in the high temperature turbine, only part of the flue gas is further expanded to vacuum and then condensed in the Rankine-like cycle, the remainder is recycled back via a compressor to the combustor, bringing its internal heat back to the combustor, thus significantly reducing the associated exergy loss to the environment. The mixing loss associated with combustion is reduced too because of the composition similarity of the streams entering the combustor. The analysis predicts that the ZE-SOLRGT system with an 18% solar heat input share has a thermal

efficiency of 50.7% and exergy efficiency of 53%, with ~100% CO₂ capture.

Acknowledgment

The authors gratefully acknowledge the support from the Chinese Natural Science Foundation Project (Nos. 51076152, 50836005) and the National Key Fundamental Research Project (No. 2010CB227301).

Nomenclature

- A = energy level, $\Delta E/\Delta H$, Eq. (10)
- CR = methane conversion ratio
- E = exergy [kW]
- H = entropy [kW]
- LHV = lower heating value of fuel [kJ/kg]
- m = mass flow rate [kg/s]
- p = pressure [bar]
- Q = heat [kW]
- R_{sm} = steam-methane mole ratio to the reformer
- R_f = fossil fuel replacement per kJ solar energy input [kJ fossil fuel/kJ solar heat], Eq. (7)
- R_{fe} = fossil fuel replacement per kJ solar exergy input [kJ fossil fuel/kJ solar heat exergy], Eq. (8)
- S = entropy [kW/K]
- SR_f = fossil fuel saving ratio, Eq. (6)
- T = temperature [°C]
- TIT = turbine inlet temperature [°C]
- W_{net} = net power output [kW]
- W_{ref} = power output of the reference system [kW]
- $X_{e,sol}$ = solar exergy input share, Eq. (4)
- X_s = steam-air mass ratio
- X_{sol} = solar heat input share, Eq. (3)
- η_e = system efficiency [%], Eq. (2)
- η_{ex} = exergy efficiency [%], Eq. (9)
- η_{sol} = solar-to-electricity efficiency [%], Eq. (5)
- η_{th} = thermal efficiency [%], Eq. (1)

Subscripts

- a = energy acceptor
- d = energy donor
- f = fuel
- rad = solar radiation
- ref = reference system
- sol = solar heat
- syn = syngas
- TIT = turbine inlet temperature
- 0 = environment state
- 1,2...29 = states on the cycle flow sheet

References

- [1] Zhang, N., and Lior, N., 2012, “Use of Low/Mid-Temperature Solar Heat for Thermochemical Upgrading of Energy, Part I: Application to a Novel Chemically-Recuperated Gas-Turbine Power Generation (SOLRGT) System,” *ASME J. Eng. Gas Turbines Power*, Accepted.
- [2] Hong, H., Jin, H., Ji, J., Wang, Z., and Cai, R., 2005, “Solar Thermal Power Cycle With Integration of Methanol Decomposition and Middle-Temperature Solar Thermal Energy,” *Sol. Energy*, **78**, pp. 49–58.
- [3] Ishida, M., and Kawamura, K., 1982, “Energy and Exergy Analysis of a Chemical Process System With Distributed Parameters Based on the Energy Direction Factor Diagram,” *Ind. Eng. Chem. Process Des. Dev.*, **21**, pp. 690–695.
- [4] Ishida, M., 2002, *Thermodynamics Made Comprehensible*, Nova Science, New York.
- [5] Jin, H., and Ishida, M., 1993, “Graphical Exergy Analysis of Complex Cycles,” *Energy*, **18**, pp. 615–625.
- [6] Dunbar, W. R., and Lior, N., 1994, “Sources of Combustion Irreversibility,” *Combust. Sci. Tech.*, **103**, pp. 41–61.
- [7] Hong, H., Jin, H., Sui, J., and Ji, J., 2008, “Mechanism of Upgrading Low-Grade Solar Thermal Energy and Experimental Validation,” *ASME Trans. J. Sol. Energy Eng.*, **130**, p. 021014.
- [8] Abdallah, H., and Harvey, S., 2001, “Thermodynamic Analysis of Chemically Recuperated Gas Turbines,” *Int. J. Therm. Sci.*, **40**, pp. 372–384.

- [9] Kesser, K. F., Hoffman, M. A., and Baughn, J. W., 1994, "Analysis of a Basic Chemically Recuperated Gas Turbine Power Plant," *ASME J. Eng. Gas Turbines Power*, **116**, pp. 277–284.
- [10] Abdallah, H., Facchini, B., Danes, F., and de Ruyck, J., 1999, "Exergetic Optimization of Intercooled Reheat Chemically Recuperated Gas Turbine," *Energy Convers. Manage.*, **40**, pp. 1679–1686.
- [11] Nakagaki, T., Ogawa, T., Hirata, H., Kawamoto, K., Ohashi, Y., and Tanaka, K., 2003, "Development of Chemically Recuperated Micro Gas Turbine," *ASME Trans. J. Eng. Gas Turbines Power*, **125**, pp. 391–397.
- [12] Han, W., Jin, H., Zhang, N., and Zhang, X., 2007, "Cascade Utilization of Chemical Energy of Natural Gas in an Improved CRGT Cycle," *Energy*, **32**, pp. 306–313.
- [13] Jericha, H., Gottlich, E., Sanz, W., and Heitmeir, F., 2004, "Design Optimization of the Graz Cycle Prototype Plant," *ASME J. Eng. Gas Turbines Power*, **126**, 733–740.
- [14] Sanz, W., Jericha, H., Bauer, B., and Gottlich, E., 2008, "Qualitative and Quantitative Comparison of Two Promising Oxy-Fuel Power Cycles for CO₂ Capture," *ASME J. Eng. Gas Turbines Power*, **130**, p. 031702.
- [15] Sanz, W., Jericha, H., Moser, M., and Heitmeir, F., 2005, "Thermodynamic and Economic Investigation of an Improved Graz Cycle Power Plant for CO₂ Capture," *ASME J. Eng. Gas Turbines Power*, **127**, pp. 765–772.
- [16] Zhang, N., and Lior, N., 2008, "Two Novel Oxy-Fuel Power Cycles Integrated with Natural Gas Reforming and CO₂ Capture," *Energy*, **33**, pp. 340–351.
- [17] Zhang, N., and Lior, N., 2008, "Comparative Study of Two Low CO₂ Emission Power Generation System Options with Natural Gas Reforming," *ASME J. Eng. Gas Turbines Power*, **130**, p. 051701.
- [18] Luo, C., and Zhang, N., 2011, "Zero CO₂ Emission SOLRGT System," Proceedings of ECOS2011, Novi Sad, Serbia, July 4–7, 2011.